1-11-2017

Novel Synthesis of a Solid Silver Oxalate Complex Used for Printing Conductive Traces.

Khushbu Zope
kz1240@rit.edu

R.I.T.

Novel Synthesis of a Solid Silver Oxalate Complex Used for Printing Conductive Traces.

by

Khushbu Zope

A Thesis Submitted in Partial Fulfillment of the

Requirements for the Degree of

Master of Science

in

Materials Science and Engineering.

School of Chemistry and Materials Science

College of Science

Rochester Institute of Technology

Rochester, NY

January 11th 2017

School of Chemistry and Materials Science College of Science

Rochester Institute of Technology

Rochester, New York

CERTIFICATE OF APPROVAL

The M.S. degree thesis of Khushbu Zope has been examined and approved by the thesis committee as satisfactory for the thesis required for the M.S. degree in Materials Science and Engineering.

Dr. Scott Williams Date

Professor, School of Chemistry and Materials Science. *Chief advisor*

Dr. Denis Cormier Date

AMPrint Center Director; Earl W. Brinkman Professor, Industrial and Systems Engineering.

Dr. Bruce Kahn Date

Director of Business Development-AMPrint Center.

Dr. Mark Irving Date

Research Professor, Industrial and Systems Engineering.

Abstract

A solid silver – ligand complex, μ-oxolato-bis(ethylenediaminesilver(I)) was developed for formulating particle-free conductive inks. The complex has approximately 47% silver content by weight, and is soluble in ink-jet compatible polar solvents. Aqueous ink formulations for the inkjet printing was developed to print uniform films on glass and polyimide substrates. When cured, printed films comprising crystalline metallic silver was determined by XRD. Optimized curing conditions were found to be 120°C for less than five minutes, which may be compatible with high throughput printing. Cured films demonstrated better adhesion on polyimide substrates than on glass. This study has improved the state of the art material used for MOD inks and provided a method for printing on a variety of flexible electronic form factors.

Acknowledgements

My most sincere and humble thanks to:

Dr. Scott Williams, for all the time and insights he has provided to guide me to be a better researcher.

Dr. Denis Cormier, for the generous support throughout the development of this thesis.

Dr. Bruce Kahn, for making the working place more welcoming by sharing his experiences.

Dr. Mark Irving, who shared his vision of making experiments more meaningful.

Dr. Thomas Smith, Dr. Ken Reed and Dr. Mandakini Kanungo, for their guidance to shape the research study.

Dr. Casey Miller and Dr. Paul Craig, for the opportunity to study Materials Science and Engineering at School of Chemistry and Materials Science, RIT.

My friends and fellow research students, for helping me without any reservations.

My parents and parents-in-law, for enduring my pangs of unconventionality.

My husband, for enriching my life with confidence to make it all possible.

Thank you.

List of Abbreviations

AgOX	Silver oxalate
DTA	Differential thermal analysis
EDS	Energy-dispersive X-ray spectroscopy
IJ-Ag	Inkjet silver MOD formulation
IR	Infra-red spectroscopy
MOD	Metal-organic decomposition (ink)
NMR	Nuclear magnetic resonance spectroscopy
NP	Nanoparticles
OLED	Organic light emitting diode
PET	Poly(ethylene terephthalate)
PI	Polyimide
RFID	Radio frequency identification
ROM	Reactive organometallic (ink)
RT	Room temperature
S-Ag	Solid silver complex
SEM	Scanning electron microscopy
ST	Surface tension
TGA	Thermogravimetric analysis
XRD	X-ray diffraction

List of Figures

List of Tables

Table of contents

Chapter 1. Introduction

As the size of conventional electronics decreases, the cost of manufacture is increasing. In this era, where technology is at our fingertips in the form of smart devices, reducing the price and weight of the electronic components is desirable. In an attempt to satisfy this demand, printed electronics are capturing industry attention for their properties of lower-cost, flexibility and lighter weight. The potential applications are sensors,[1, 2] transistors,[3, 4] photovoltaics,[5, 6] displays,[7] supercapacitors,[8] organic light emitting diodes (OLED)[9], radio frequency identification (RFID) tags[10] and energy harvesting devices.[11] Decades of effort have resulted in material and process developments.[2, 5, 7, 12-16] Translating these developments from the lab bench to the print production floor however, requires tuning the materials to the demands made by the large scale printing process and workflow.[17] Particular effort has been made toward printing ink formulations to produce electronic traces, interconnects and contacts.[18-21]

Silver ink formulations have been extensively studied in the form of nanoparticles[21], MOD[22] (metal-organic decomposition) inks for inkjet printing, and in the form of pastes[23] for screen printing. To overcome the printing process limitations imparted by particle-based dispersions, solution-phase inks that produce a metal conductive trace upon thermal activation, known as precursor inks or metal-organic-decomposition (MOD) inks, have been developed.[20, 21, 24] Similarly, copper,[25] carbon nanotubes,[4] graphene[26] and conducting/ semiconducting polymers[27-29] are considered for printing functional devices. Substrates used for printing such devices include paper,[30] polyimide films,[31] polyesters[32] polycarbonate,[33] polyether imide and polyacrylate.[34]

Silver MOD ink technologies vary primarily by the ligands used to solubilize and stabilize the metal. Early work involved using silver carboxylate soaps that were soluble in organic solvent systems optimized for ink jet printing. [18, 35-37] Although these systems produced silver traces with conductivities approaching that of bulk silver, the nominal curing temperatures and times were too high to be viable in a production workflow. Lowering the curing and/or sintering temperature and reducing processing time required research into alternative silver-ligand complexes and solvent additives. [22, 24, 38, 39] With many of these alternative approaches, nominal conductivity was only achieved by further processing the samples at longer times or higher temperatures.

Particle-based metal inks and silver film conductivity of reactive inks have been improved by increasing the silver loading fraction. One approach was to select ligands possessing multiple silver binding sites, thereby increasing the available reducible silver concentration while still maintaining ink stability. Silver oxalate[22, 23, 40] and silver citrate[41] are two examples of silver – ligand complexes that were found to have excellent ink stability properties as well as promoting silver reduction upon thermal activation. These material improvements, however, have yet to gain adoption because they would disrupt current production processes.

In this study, we present an improved synthetic approach using silver oxalate and optimized ink formulations. The approach includes these following factors: (i) high silver content silver oxalate salt which is easily reduced to elemental silver, (ii) complexing agents to stabilize the silver salt, (iii) water as solvent, (iv) long term stability of the ink in solid form and (vi) curing at 130°C for two minutes.

Chapter 2. Literature Review

2.1 Printed Electronics

Printed electronics have promising applications for future consumer electronics. Their flexibility and lightweight characteristics meet the emerging application needs in displays,[42] healthcare,[43] energy harvesting,[11] wearable[44] and human machine interface technologies.[13] Advantages[44] of integrating printed electronics with various applications are listed below.

1. Low-cost fabrication promotes economies of scale which decreases the cost per part as the level of production increases. If low cost sensor tags are available in the form of printed electronics, it will be applicable to a large number of products.
2. Similar fabrication technology can be used for different applications by changing the design of the trace to be printed. Tailor made designs are easily offered by such printing processes.
3. Printing on flexible substrates opens new doors for applications. Bendable and stretchable substrates, for example, are necessary for wearable sensors. Some wearable sensors can directly go on to the skin since they are flexible.
4. Seamless integration is possible due to the compatibility of printing process and materials with various substrates. Materials developed for a specific printing processes can be utilized to print on alternate substrates with slight modifications.
5. Emerging applications are opening new fields. Printed electronics are emerging as sensors in healthcare monitoring units providing non-invasive tests, and replacing patient-unfriendly invasive tests.

2.2 Inks and Substrates

A printing ink comprises at least one active ingredient, and a suitable vehicle for the selected printing process. The active ingredient provides the function of the printed device, e.g. electrical conductivity or sensing. The ink vehicle is generally a mixture of ingredients responsible for precise roles such as (a) active ingredient solubilizing agent, (b) reducing agent, (c) humectant, (d) stabilizing agent for nanoparticles (if any), or (e) rheology modifier. A detailed account of recently explored ink formulations are summarized in ***Table 1***.

Table 1: Recent advances in materials and processes for printed electronics.

Type of ink	Formulation	Substrate	Printing process	Year	Application	Ref.
Silver MOD[a]	Silver oxalate, ethylamine, ethyl alcohol, ethylene glycol	Polyimide	Inkjet	2015	Inkjet printing	Dong et al.[22]
Silver MOD	Silver acetate, ammonium hydroxide,	Poly(ethylene terephthalate), polyimide, glass	Inkjet	2012	High-conductivity features	Walker et al.[24]
Silver ROM[b]	Silver hexafluoroacetyl-acetonate cyclooctadiene, toluene, isopropyl alcohol	Glass	Inkjet	2016	Atomic Layer Deposition (ALD)	Black et al.[39]
Copper /Silver MOD	Copper(II) acetate monohydrate, silver oxide, ammonia solution, di-ethanolamine	Glass, polyimide	Spray pyrolysis	2016	Conductive films	Suren et al.[45]
Silver NP[c]	Silver nanowires, zinc oxide	Poly(ethylene terephthalate)	Rotary screen printing	2015	Semi-transparent electrodes	Angmo et al.[46]
Silver MOD	Silver carbonate, glycol, water, isopropyl amine	Polyimide	-	2012	Conductive traces	Chang et al.[47]

Type of ink	Formulation	Substrate	Printing process	Year	Application	Ref.
Silver NP	Commercial silver nanoparticles inks: organic base and aqueous base	Substrate with polymeric receiving layer, substrate with inorganic micro-porous receiving layer	Inkjet	2015	Frequency selective surfaces (FSS), RFID tags	Sanchez-Romaguera et al.[10]
Silver MOD	Silver acetate, ethanolamine, ethanol, reducing agents (ethylene glycol, acetaldehyde, formic acid, dimethylformamide or glucose)	PDMS layer on PET adhered to glass	Pattern created by laser etching	2013	Micro-electronics	Tao et al.[48]
Silver MOD	Silver carbonate, glycol, water, isopropyl amine	Polyimide	-	2012	Conductive traces	Chang et al.[47]
Silver NP	Silver nanoparticles [from silver nitrate, sodium borohydrate and capping agents - poly (vinylpyrrolidone), polyaniline, L-cysteine or Oleic acid] dispersed in ethanol	Poly(ethylene terephthalate)	-	2012	Printable electronics	Li et al.[49]
Silver NP	Silver nanoparticles (from silver acetate, toluene, phenyl hydrazine and stabilizing agents: 1-hexadecylamine or 1-dodecylamine) dispersed in cyclohexane	Glass, SiO_2 surface	Spin coating, mask-assisted microcontact printing	2005	Transistors	Li et al.[50]
Silver/ Copper NP[d]	Silver nitrate, copper nitrate, hydrazine hydrate, polyacrylic acid sodium salt	Glass	Inkjet printing	2009	Conductive traces	Grouchko et al.[51]

[a] = Metal-organic decomposition, [b] = Reactive organometallic, [c] = nanoparticles and [d] = nanoparticles of copper core and silver shell.

2.2.1. Silver MOD:

MOD stands for metal-organic decomposition. In MOD inks (***Figure 1***), a metal ion is coordinated to an electron donating (typically organic) molecule through a lone pair of electrons. This metal containing molecular complex usually portrays enhanced solubility and stability in the chosen ink vehicle. In addition, the complexing molecule is selected in such a way that the metal becomes highly conductive after thermal decomposition of the organic content.

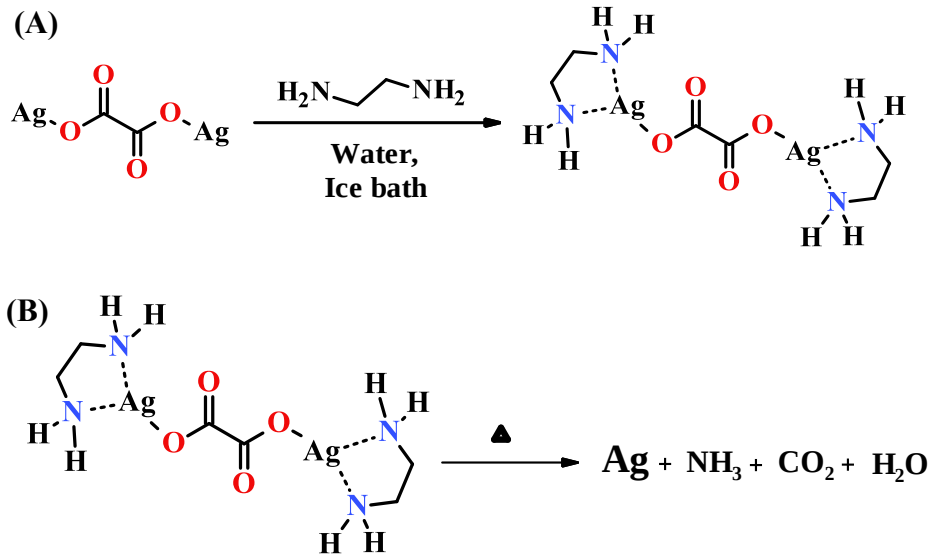

Figure 1: Proposed reaction schemes for solid silver complex formulated for this study (A) formation of solid silver (S-Ag) complex - μ-oxolato-bis(ethylenediaminesilver(I)) from silver oxalate and ethylene diamine in water and (B) thermal decomposition of the S-Ag complex.

Silver is solvated in these ink formulations, giving the formulations better stability than that of nanoparticle inks. Unlike MOD inks, particulate inks can encounter problems of nozzle clogging due to particle agglomeration. Recently, Dong et al.[22] used silver oxalate salt to formulate MOD ink for inkjet printing applications. This ink was reported to be

stable for several months when stored at temperatures below 10°C in the dark. The curing conditions were 150°C for 30 minutes. In 2012, Walker et al.[24] formulated silver MOD ink with silver acetate as the precursor. This ink formulation took 15 minutes to cure at 90°C and the conductivity reported was equivalent to bulk silver.

Similar to MOD inks, silver ROM (Reactive Organometallic) inks were explored to avoid the curing process after printing. Black et al.[39] demonstrated a sinter-free process of silver ROM ink on a heated substrate to produce conductive films.

2.2.2. Silver nanoparticle inks:

Recently, multiple scientific studies reported the electrical device fabrication using silver nanoparticles instead of the vacuum deposition process.[29] In one of the studies, nanoparticles of 10 nm diameter were stabilized by long chain 1-alkylamines.[50] Li et al.[49] compared the conductivity obtained from silver nanoparticles using different capping agents. The study indicated that silver nanoparticles/poly (vinylpyrrolidone) showed better conductivity than silver nanoparticles systems having other capping agents such as, polyaniline, L-cysteine or oleic acid. Sanchez-Romaguera et al.[10] investigated the correlation between silver nanoparticles, substrates and sintering methods and stated that the choice of sintering process was limited by the size of nanoparticles and the type of substrate used.

Like other various studies, printing with a silver nanowire containing ink has been demonstrated by Angmo et el.[46] Silver nanowire films thus printed were transparent as required for solution-processed solar cells and other optoelectronic devices. .

2.2.3. Hybrid inks:

Suren et al.[45] fabricated a continuous film made of silver and copper particles. These hybrid material films were made by spray pyrolysis of solution based ink, followed by annealing at 200°C for 25 mins in an inert atmosphere of nitrogen. Core-shell nanoparticles having copper as core and silver as shell have been formulated by Grouchko et al.[51] Upon heating, however, the silver shell breaks open to expose and oxidize copper, compromising the electrical conductivity of the printed patterns.

2.3 Printing Processes

Inkjet printing is the most widely explored technique in current research explorations of printed electronics.[52] Inkjet printing[53] provides the controlled ability to deliver drops (of picoliter volume) on demand. Most commercial printers use piezoelectric ejection for the nozzels.[54]. The ejection chambers contain piezoelectric material, which contracts and expands with applied AC voltage to create droplets. These droplets are fired towards the substrate directed by the nozzles. Adhesion and spreading of the droplets onto the substrate is determined by the substrate surface energy and ink surface tension and rheology.

Apart from inkjet printing, other widely explored printing techniques are flexography, screen printing, gravure printing, aerosol-jet printing and offset lithography.[15] High viscosity paste inks are spread over a patterned mesh with uniform speed in screen printing. In this case, print resolution is limited by the mesh size. On the other hand, gravure printing provides good resolution, but is limited to large sized batches and long production runs without the ability to produce low volumes affordably.

Chapter 3. Objectives

Silver metal was the focus of this study due to its moderate reduction potential and high conductivity in the metallic state. MOD formulations were preferred over particulate formulations to improve ink stability. Nanoparticles in the particulate ink, for example, can agglomerate and show poor stability. These agglomerates can also block the print-head nozzles during the printing process.

In MOD inks, dissolved metal-ligand complex remains in solution for a long period of time. MOD ink stability is limited by the stability of metal-ligand complex. Taking the metal-ligand complex out of the solution form to a solid state complex, would enhance the stability further. This solid complex could be used by dissolving it in the appropriate vehicle when needed for printing.

Improving the current state of the art for materials and process parameters of MOD inks were the primary goals of this research study. The two main aspects of these goals include:

1. Development of a new solid silver complex having the active component as a solid material that could be dissolved into an ink vehicle when needed, and
2. To provide the curing conditions compatible with high throughput processing conditions.

The materials selected for the metal-ligand complex were silver oxalate and ethylene diamine. Silver oxalate is 71% w/w silver. Silver oxalate thermally decomposes to silver and carbon dioxide.[40] Ethylene diamine is a bi-dentate metal ligand and boils at a low temperature (116°C). Having less organic content in the metal-ligand complex should make the curing (reduction to silver) process easier and faster as the energy and time

required to combust the organic content to carbon dioxide is directly proportional to the amount of organic content.

Chapter 4. Experimental

4.1 Materials

All the chemicals used were analytical grade. Silver nitrate, oxalic acid dihydrate, ethylene diamine and isopropyl alcohol were purchased from Acros Organics, US. These chemicals were used without any further purification steps. Glass microscope slides (from Corning Incorporated USA) and Kapton® film (DuPont USA, polyimide, 0.1 mm thick) were used as substrates.

4.2 Procedures

Silver Oxalate Synthesis.

The silver oxalate synthesis procedure was adapted from a previously published procedure[55]. Oxalic acid (0.5 M, 30 ml) solution was added to a silver nitrate solution (0.5 M, 50 ml). The white precipitate of silver oxalate thus obtained was filtered and washed with distilled water. Silver oxalate was then dried at 60°C for six hours and stored in the dark at room temperature.

Solid Silver (S-Ag) Ink Formulation.

Ethylene diamine (0.726 ml, 10.864 mmol) was dissolved in 1.2 ml of distilled water. Silver oxalate (1.1 g, 3.621 mmol) was then added to this solvent mixture at intervals over the period of five minutes. An excess of isopropyl alcohol (15ml) was added to this liquid ink mixture. The precipitated silver complex was filtered and washed with small volumes of isopropyl alcohol. The solid ink was then dried at RT under vacuum for four hours and stored in an amber colored storage bottle below 4°C.

Inkjet Printable Liquid Silver (IJ-Ag) Ink Formulation.

The silver complex proposed to be μ-oxolato-bis(ethylenediaminesilver(I)) (S-Ag) ink solid (2.5 g) was dissolved in distilled water (2.5 ml). Rheology and surface tension were adjusted to 29.6 N/m and 15-18 mPa·s respectively by adding isopropyl alcohol (0.3 ml) to the mixture. The ink jet (IJ-Ag) ink was filtered through 0.2 μm syringe filters before printing.

Inkjet Printing.

IJ-Ag ink was printed on glass microscope slides and Kapton® films with a Dimatix printer (DMP-3000 by Fujifilm USA). The print-head temperature was set to 25°C and the print platen was kept at room temperature while printing. Kapton films and glass substrates were cleaned with isopropyl alcohol before printing. The stand-off distance from print-head to substrate was set to 800 μm for Kapton® film and 1200μm for the glass substrate. Printed patterns were cured at temperatures ranging from 90°C to 150°C on a hot-plate to achieve good conductivity.

S-Ag and IJ-Ag Characterization.

IR: Silver oxalate and S-Ag complex were studied by infrared spectroscopy (Shimadzu IR Prestige-21 with ATR).

NMR: S-Ag complex and oxalic acid were analyzed by ^{13}C NMR (Bruker Avance DRX 300) in deuterated water (D_2O).

Surface tension of IJ-Ag ink was measured using a Contact Angle Goniometer and Tensiometer (Model 250, Rame-hart, USA) using the pendant drop method.

Stability studies of the S-Ag complex and IJ-Ag ink were performed for 60 days at 4°C and RT.

Thermogravimetric analysis (TA Instruments, Model: Q500) was performed for Silver oxalate, S-Ag complex and IJ-Ag ink. The sample (~ 8mg) was heated from room temperature to 300 °C at a 5°C/min rate.

Imaging: Surface morphology and thickness of the printed films were measured using a scanning electron microscope (TESCAN FESEM).

XRD: The X-ray diffraction pattern of the film was recorded on a RIGAKU Dimax-II using Cu Kα, 0.15418 nm wavelength.

Chapter 5. Results and Discussion

5.1 Silver Oxalate

Silver oxalate was selected because it contains the largest silver weight fraction (70% silver by mass). Silver oxalate[40] degradation has been comprehensively studied by Boldyrev et al. who showed that silver oxalate thermally decomposes to produce silver metal and carbon dioxide. Boldyrev et al. also demonstrated that the silver oxalate decomposition depends upon the silver oxalate preparation method. Silver oxalate was prepared by three different methods (***Table 2***) and thermally decomposed using the same heating rate.

Table 2: Different methods of silver oxalate (AgOX) preparation.

AgOX batch	Silver nitrate	Oxalic Acid	Mixing
AgOX17	0.5 M, 100 ml (50 mmol)	0.5 M, 60 ml (30 mmol)	Oxalic acid poured in silver nitrate
AgOX18	0.2 M, 100 ml (20 mmol)	0.1 M, 100 ml (10 mmol)	Simultaneous pouring
AgOX19	0.1 M, 100 ml (10 mmol)	0.05 M,100 ml (5 mmol)	Simultaneous pouring

These three original batches showed differences in their thermal decomposition profile (***Figure 2A***). The onset of the decomposition step was observed at 130°C, 142°C and 168°C for AgOX18, AgOX19 and AgOX17, respectively.

Inks were formulated with the respective AgOX batch using ethylene diamine as a complex. Ethylene diamine (0.726 ml, 10.864 mmol) was dissolved in 1.2 ml of distilled water and subsequently, silver oxalate (1.1 g, 3.621 mmol) was added to the mixture. Inks

formulated with the different AgOX batches showed the same thermal decomposition profile (***Figure 2B***). Original batch method of AgOX 19 was selected as the preferred method for the ease of preparation.

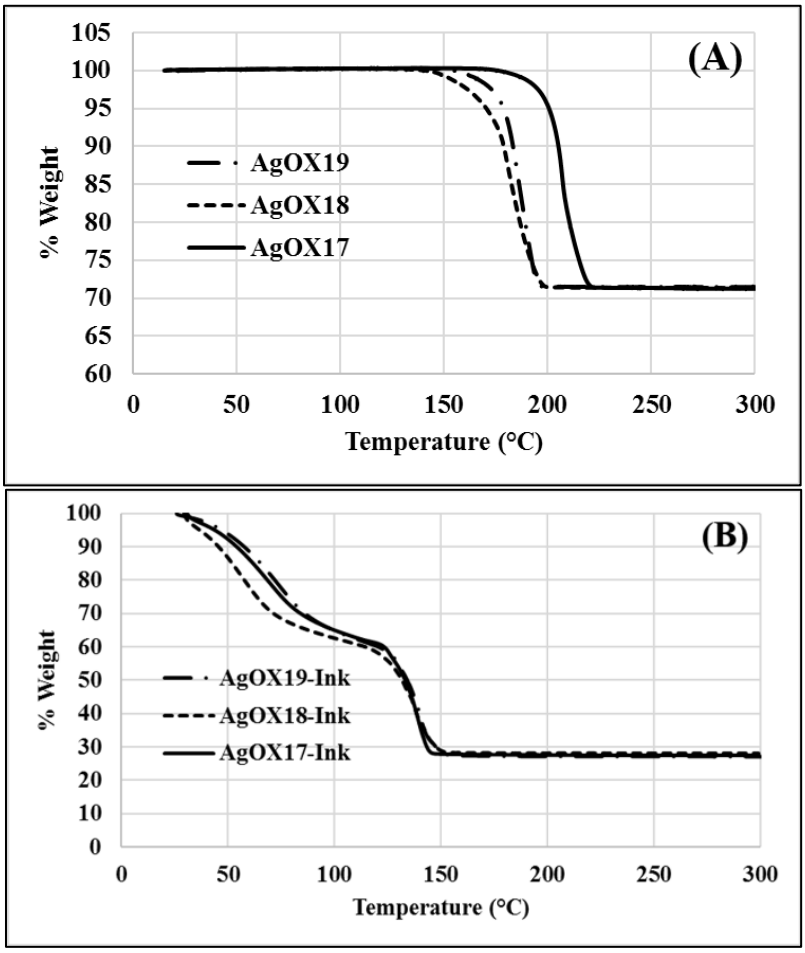

Figure 2: Thermogravimetric analysis of (A) silver oxalate batches prepared from different methods and (B) their respective ink formulations. Heating rate= 5°C/min.

5.2 Solid Silver Complex (S-Ag)

Sparingly soluble silver oxalate was found to dissolve in the presence of excess nitrogen containing complexing agents. Nitrogen containing Lewis bases increase the solubility in polar solvents by complexation.

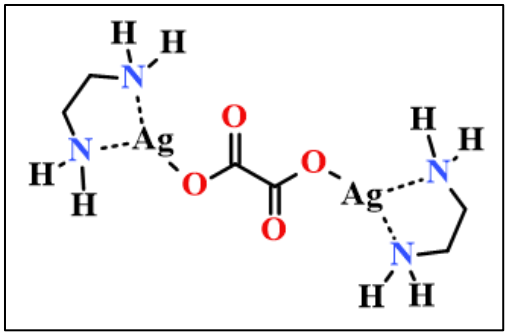

***Figure 3: Proposed structure of S-Ag complex* - μ-oxolato-bis(ethylenediaminesilver(I)).**

As a result, water was used as a solvent to solubilize the complex of ethylene diamine and silver oxalate. To get this complex from liquid (solubilized) to solid form, isopropyl alcohol was added to precipitate the solid silver (S-Ag) complex, μ-oxolato-bis(ethylenediaminesilver(I)).

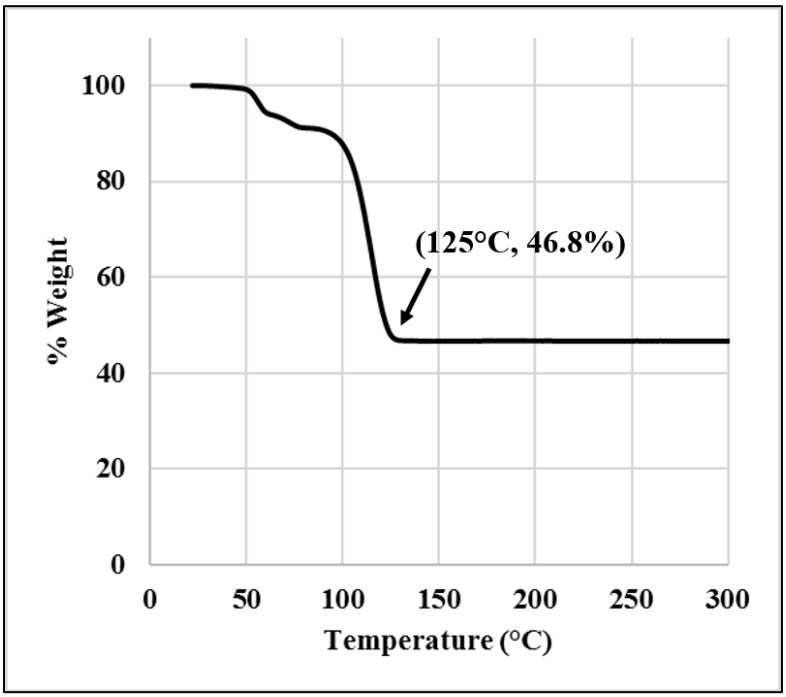

Figure 4: TGA of S-Ag indicating the silver content of 46.8%w/w (heating rate =5°C/min).

TGA of the S-Ag complex (***Figure 4***) showed that the amount of silver was 46.8% w/w which is very close to the theoretical silver content value of 51% w/w. The difference of the solid content from theoretical value may be due to impurities or residual solvent. The initial loss below 70°C could be due to trace amounts of solvent. The S-Ag complex decomposed at a lower temperature (125°C) than silver oxalate (195°C, ***Figure 2A***) using the same heating profile.

IR and NMR spectroscopies were performed to confirm the formation of the μ-oxolato-bis(ethylenediaminesilver(I)) (S-Ag) solid complex. Coordination with ethylene diamine (electron donating moiety) would exhibit peak shifts. IR and NMR spectra were studied for the original and complexed characteristic peaks to confirm the formation of solid silver complex.

In IR spectra, the O-Ag stretching peak was found by silver oxalate and by S-Ag complex at 410 cm^{-1} and 340 cm^{-1} respectively[54] (***Figure 5*** and ***Table 3Table 3***). Peak shifts to higher vibrational frequencies (lower wavenumber) indicate complexation of the electron donating moiety.[56, 57] Shorter C-C bond stretching frequencies also indicates the conjugation of ethylene diamine to silver.

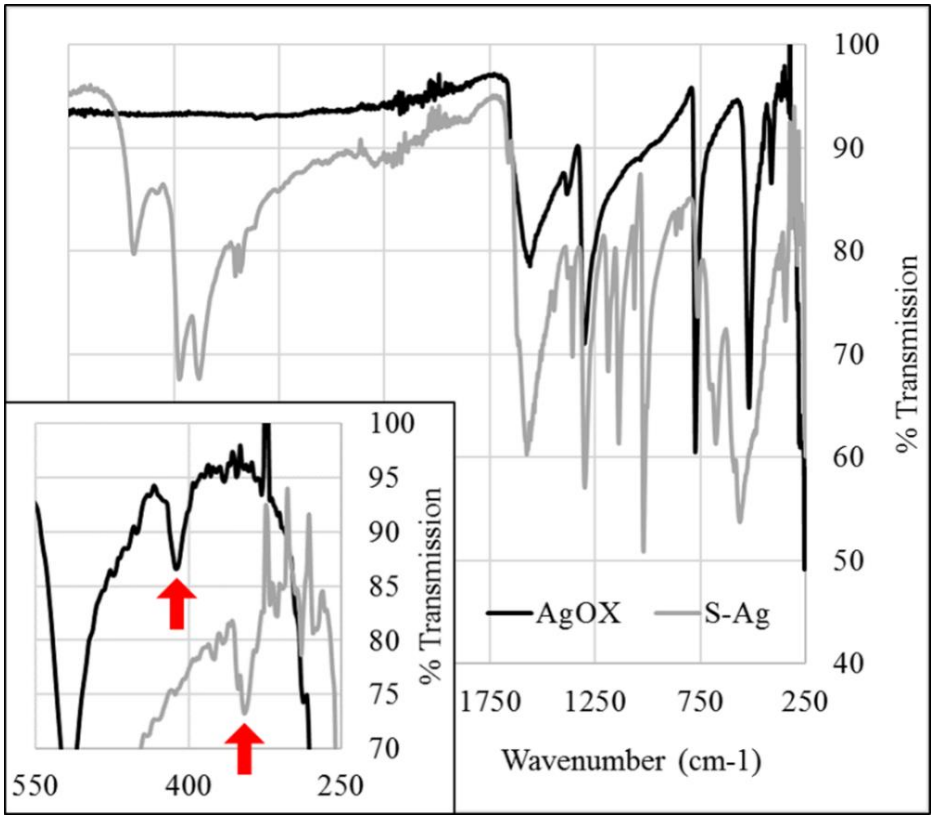

Figure 5: IR spectroscopy (A) solid complex (S-Ag) and silver oxalate (AgOX), (B) peak at 410 cm^{-1} of O-Ag bond and peak at 340 cm^{-1} of O-Ag bond conjugated with amine group from complexing agent.

Table 3: Interpretations of IR peaks. [56, 57]

Wavenumber (cm-1) and intensity [a]		**Assignments** [b]
S-Ag	*AgOX*	
1552 (s)	1556 (m)	υ_{as} (O─C═O)
1355 (m)	1375 (w)	υ_{s} (C─C)
1294 (s)	1300 (s)	υ_{s} (C─O), δ (O─C═O)
754 (m)	771 (s)	δ_{as} (O─C═O), υ_{s} (Ag─O)
-	515 (s)	δ (O─C═O)
340 (m)	410 (m)	υ (Ag─O)

[a] s = strong, m = medium. w = weak; [b] υ_s = symmetric stretching, υ_{as} = Antisymmetric stretching, δ_s = symmetric bending, δ_{as} = antisymmetric bending.

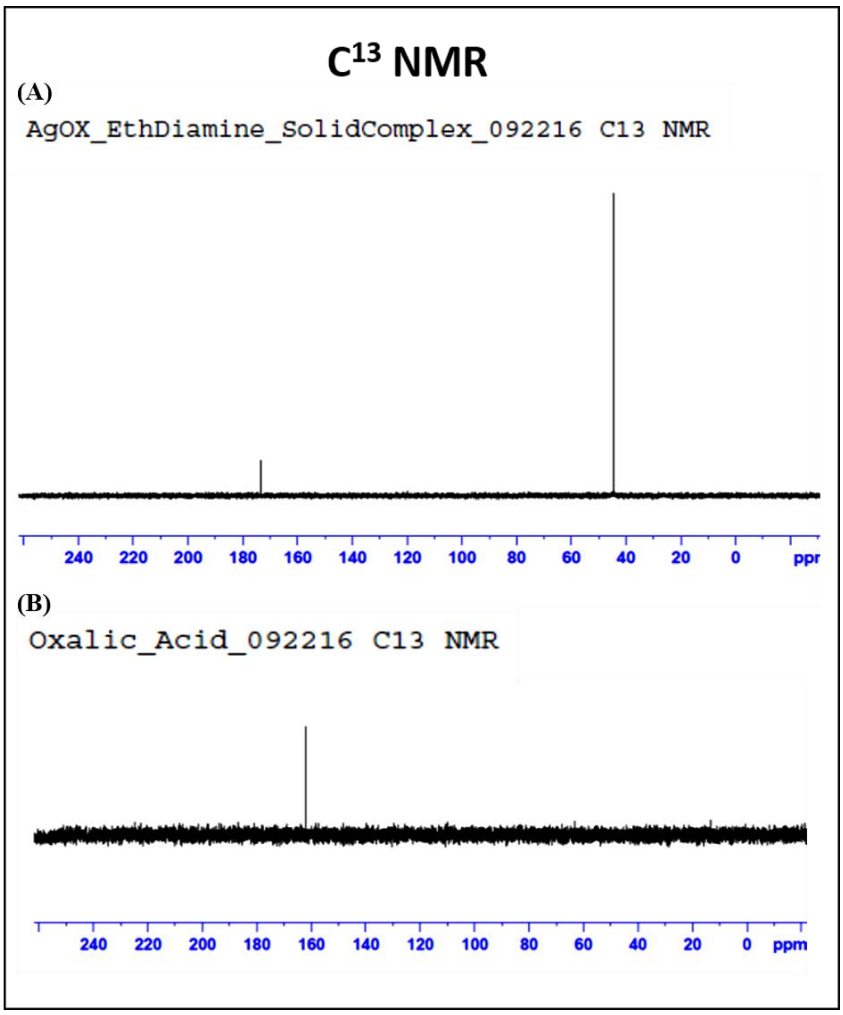

Figure 6: C13 NMR of (A) S-Ag and (B) oxalic acid.

C^{13} NMR spectra of S-Ag complex and oxalic acid were measured (see ***Figure 6***). Silver complexation to oxalic acid is expected to result in a down-field shift as shown in ***Figure 6***A, when compared with free oxalic acid (***Figure 6***B). The presence of a 44ppm C^{13}peak was assigned to the equivalent carbons on the ethylene diamine moiety (***Figure 6***A).

5.3 Inkjet Formulation

MOD ink (IJ-Ag) was formulated from S-Ag using water as the solvent. Isopropyl alcohol was used to adjust the surface tension of the formulation. The pendant drop method was

used to measure the surface tension of the formulated ink. It was consistently found to be about 30 N/m. The low surface tension assisted printing with the inkjet printer.

To understand the thermal changes during the thermal decomposition of the ink, DTA and TGA were performed (***Figure 7***). The heating rate was 2°C/min.

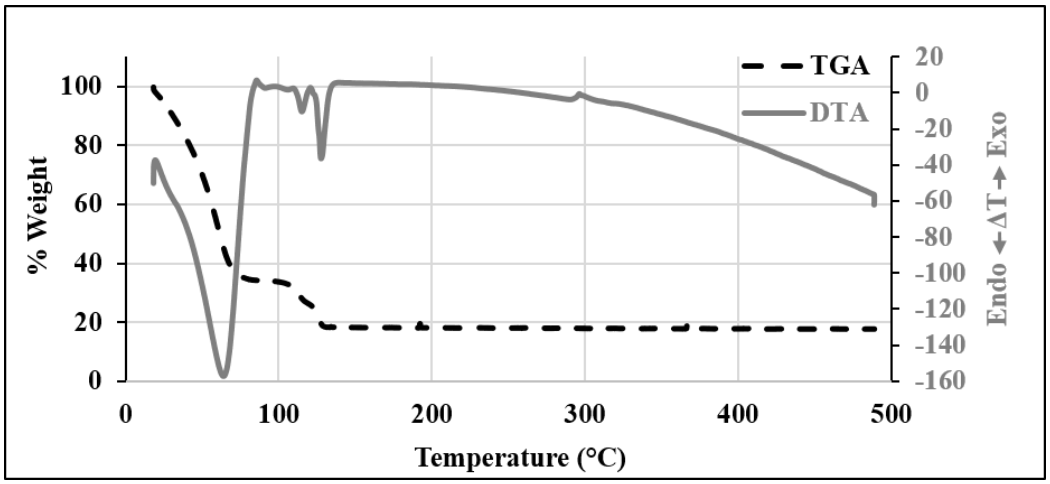

Figure 7: DTA-TGA of ink formulation.

According to the DTA-TGA data, the last endothermic peak was observed at 121°C, indicating that ink can be cured at 121°C. The endothermic peak near 300° C was considered to be an instrument anomaly, as the expected change in weight for this endothermic drop was absent on the TGA curve.

Printed silver film curing was carried out at three different temperatures: 90°C, 120°C and 150°C. As expected, less time was required to completely cure the film at higher temperatures. At 90°C, for example, the required time to cure the film was 15 minutes (***Table 4***). The films were determined to be completely cured when the simple two-point electrical resistance reached zero or no longer changed. Four-point probe measurements will be used in future studies.

Table 4: Curing conditions.

Curing temperature	Required time
90°C	15 minutes
120°C	3 minutes
150°C	Less than a minute

Curing directly at higher temperature created a non-uniform film due to rapid evaporation and rapid decomposition of the ink components (***Figure 8***). Thus, to get uniformly cured film, printed patterns were heated at 90°C for one minute and then at 120°C for three minutes.

The solid content of the ink formulation was determined by thermogravimetric analysis. The samples were heated from room temperature to 500°C using a 5°C/min heating rate. Thermal decomposition of the ink occurred in two stages (***Figure 9***). The first stage was due to solvent evaporation up to 100°C. The second stage was due to the reduction of the silver complex to metallic silver. The solid content of the ink was determined to be 21.6% w/w.

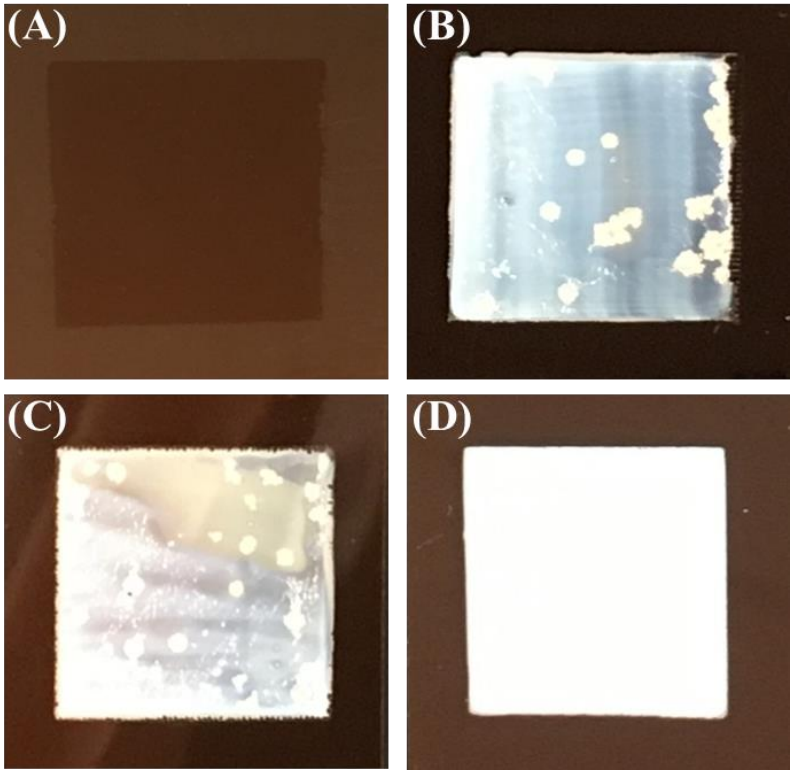

Figure 8: Curing conditions (A) printed square shaped film before curing, (B) cured at 120°C for 3 minutes, (C) cured at 150°C for 1 minute and (D) cured at 90°C for 1 minute and then at 120°C for 3 minutes.

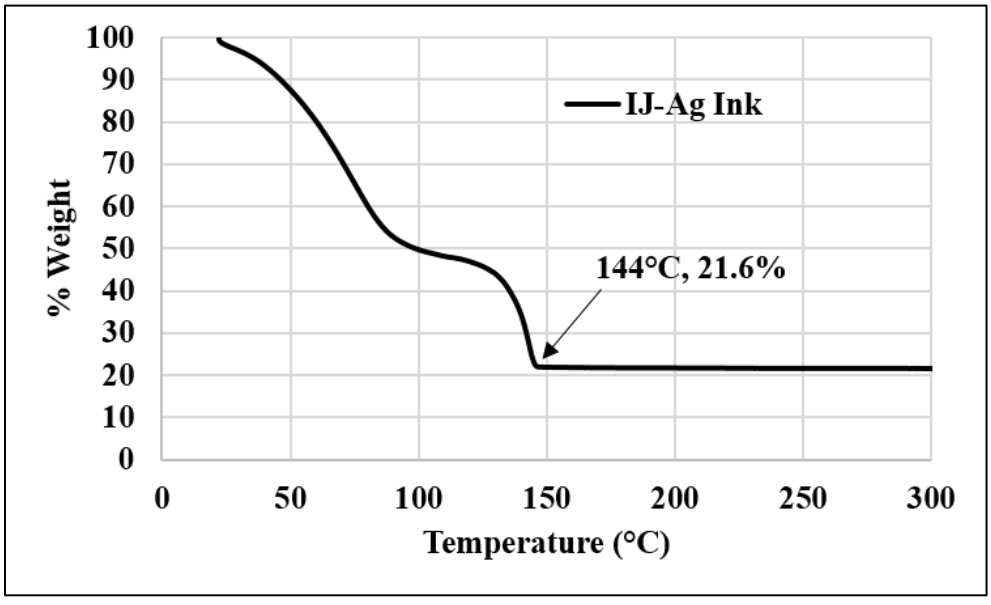

Figure 9: TGA of IJ-Ag ink formulation (heating rate 5°C/min).

5.4 Stability Studies

Stability studies were carried out for the S-Ag complex and the IJ-Ag ink formulation. Samples were stored in the dark at room temperature and at temperatures below 4°C. After three days at room temperature, the S-Ag complex powder appeared brown in color (***Figure 10B***). Below 4°C, it remained visually unchanged and stable at least for 60 days (***Figure 10C***).

Similarly, the IJ formulation appeared unchanged when stored below 4°C for 60 days. The ink solution turned grey slowly, presumably by forming particles of metallic silver at room temperature.

(A) Day 0 at RT | (B) Day 3 at RT | (C) Day 60 below 4°C

Figure 10: Stability of S-Ag complex (A) immediately after the preparation and drying, (B) After storing at 25°C for 3 days, (C) stored below 4°C for 60 days.

As expected, the IJ-Ag ink formulation also showed better stability below 4°C than that at room temperature. While stored at room temperature, silver from the ink formulation was reduced to grey colored silver particles (***Figure 11B***), which precipitated over time. Below 4°C, ink was stable over 60 days (***Figure 11C***).

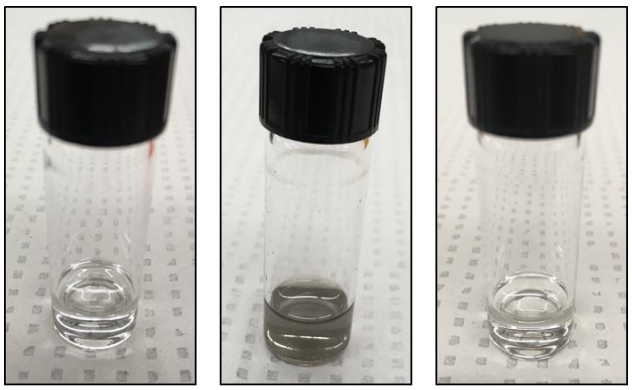

(A) Day 0 at RT (B) Day 10 at RT (C) Day 60 below 4°C

Figure 11: Stability of the ink formulation (A) stable ink immediately after the preparation of the ink, (B)unstable ink at 25°C for 10 days, (C) stable ink stored at temperature below 4°C for 60 days.

5.5 Film Characterization

Cured films were characterized by SEM imaging to study the morphology and the structure at the micro/nano scale (***Figure 12***). The films were uniform throughout (***Figure 12A***) at

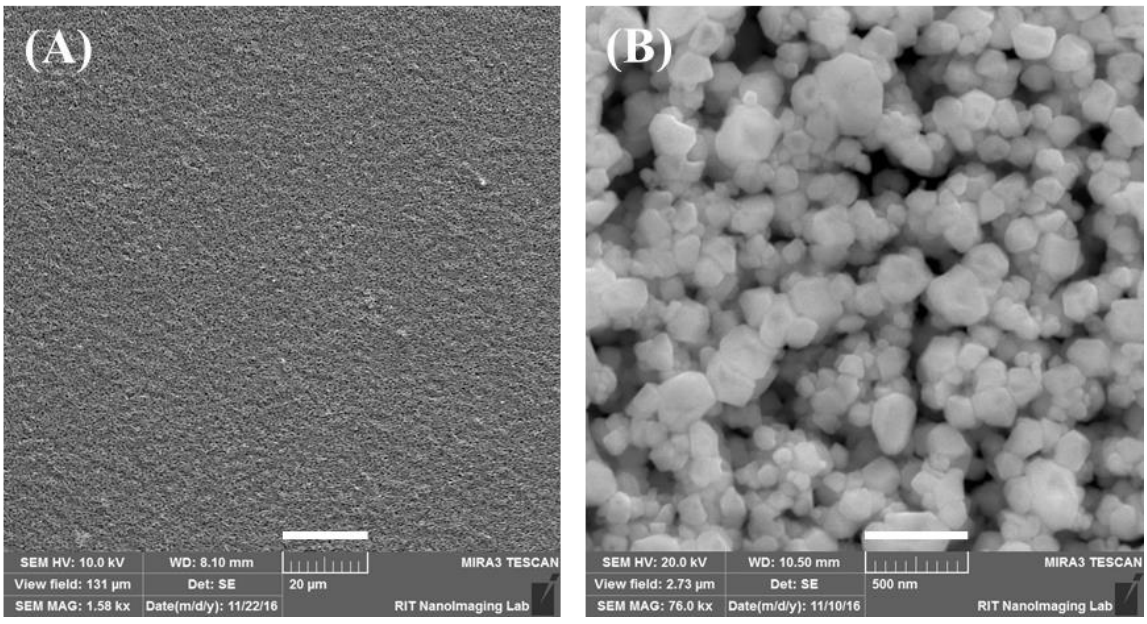

Figure 12: SEM images of the printed films cured at 90° for one minute and at 120°C for three minutes. Scales indicated are (A) 20 µm and (B) 500nm.

the micron scale. At the nanoscale, particles ranging from 100 nm to 500 nm were observed. As shown in ***Figure 12B***, significant silver grain connectivity was observed. The observed particles can be correlated with the two stages of curing: nucleation and growth. The printed and optimally cured film was cut with a sharp blade through the film and substrate. The cross-sectional view (***Figure 13***) facilitated the measurement of film thickness. Arithmetic average of the three measurements indicated that the silver film, printed on Kapton®, was 3.36 µm thick.

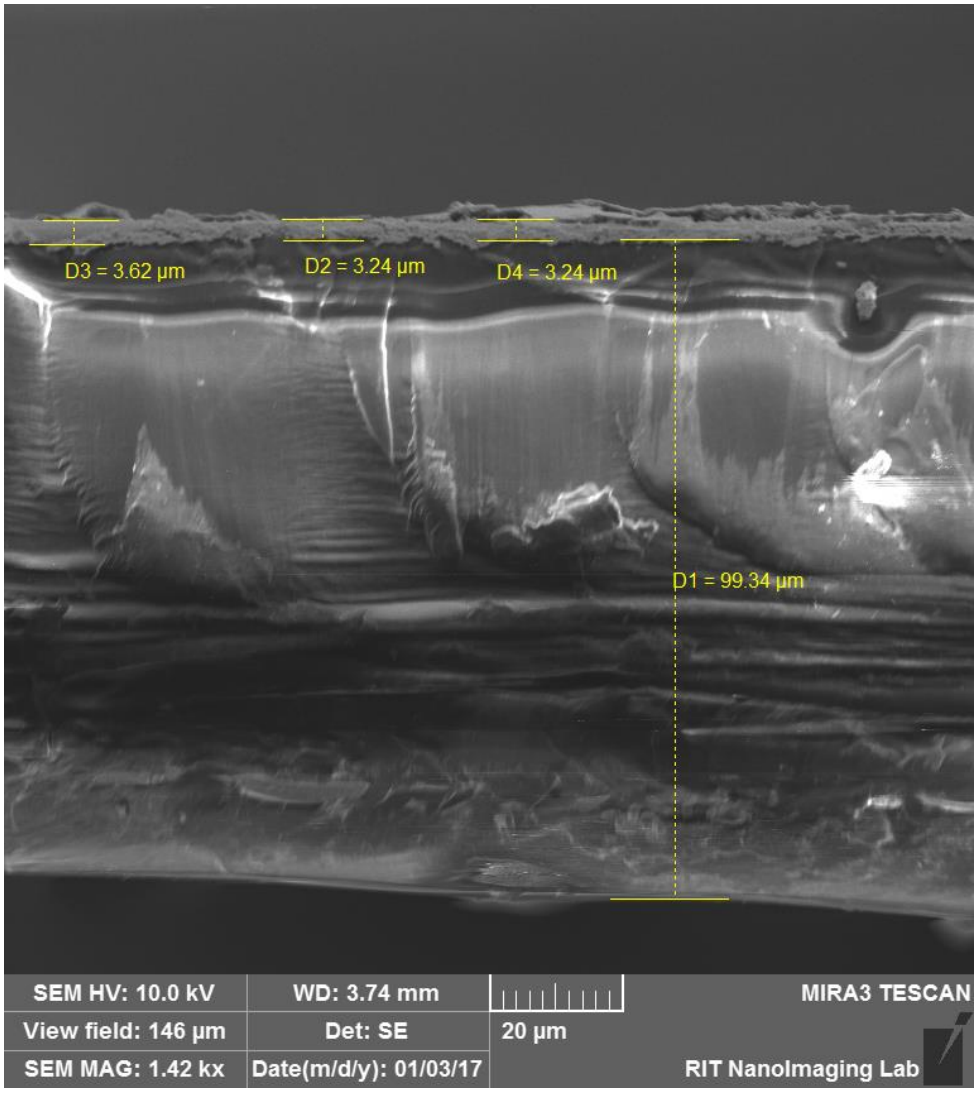

Figure 13: Cross-sectional view of the printed film along with the substrate under SEM.

The printed film was also studied by XRD to determine its crystallographic nature (***Figure 14***). As expected, conducting silver films were found to have a metallic silver, FCC crystalline structure.[58]

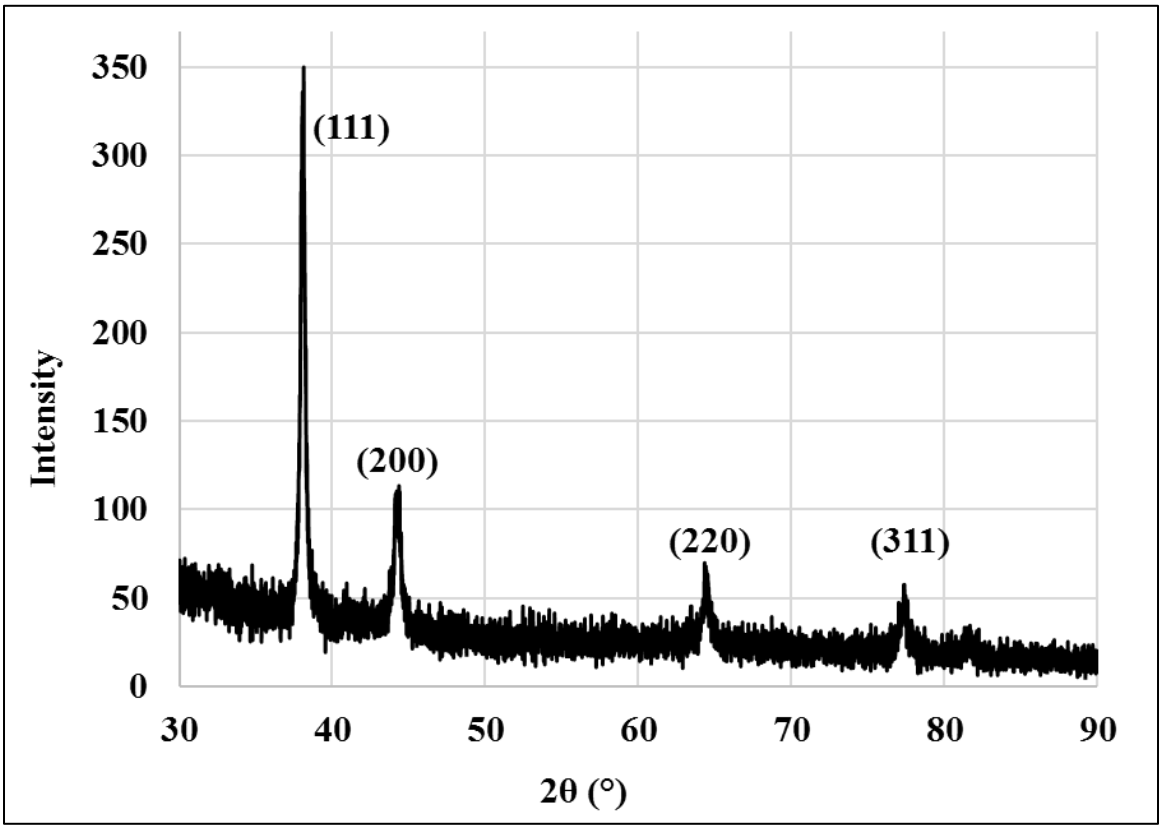

Figure 14: X-ray diffraction pattern for printed and cured silver film using IJ-Ag ink.

The elemental content of the film was analyzed by energy dispersive x-ray spectroscopy (EDS). As anticipated by the electrical conductivity, cured films were primarily composed of metallic silver as represented in ***Figure 15***. Organic matter (in the form of carbon content) was present in the films, but less abundant than silver (***Figure 15***, inset). Nitrogen and oxygen however, were found to be essentially absent.

The adhesion of the film on both substrates (glass and polyimide) was tested using a tape test. The method for the tape test was similar to ASTM standard D3359-09e2.[59] The adhesion on polyimide was greater than the adhesion on glass (***Figure 16***). However, the upper layer of film on the polyimide substrate was chipped off, indicating poor film cohesion.

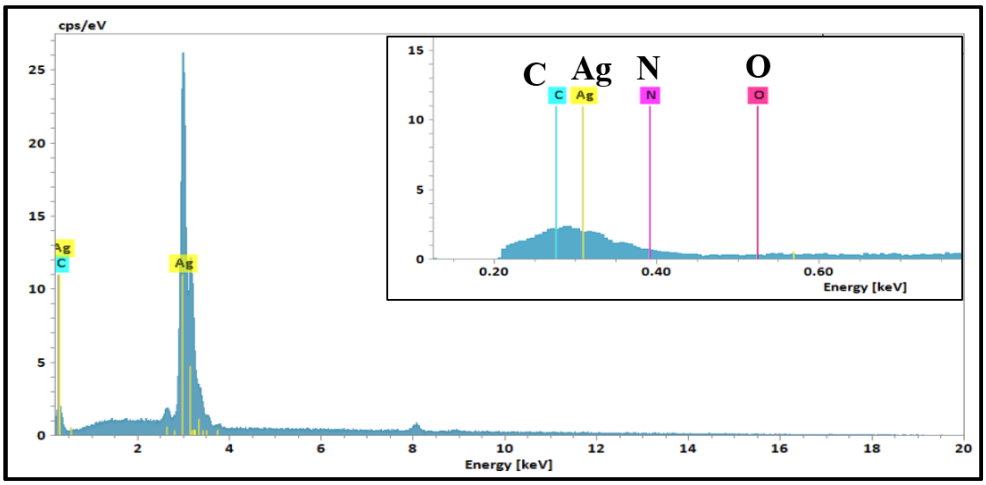

Figure 15: EDS spectrum of printed silver film.

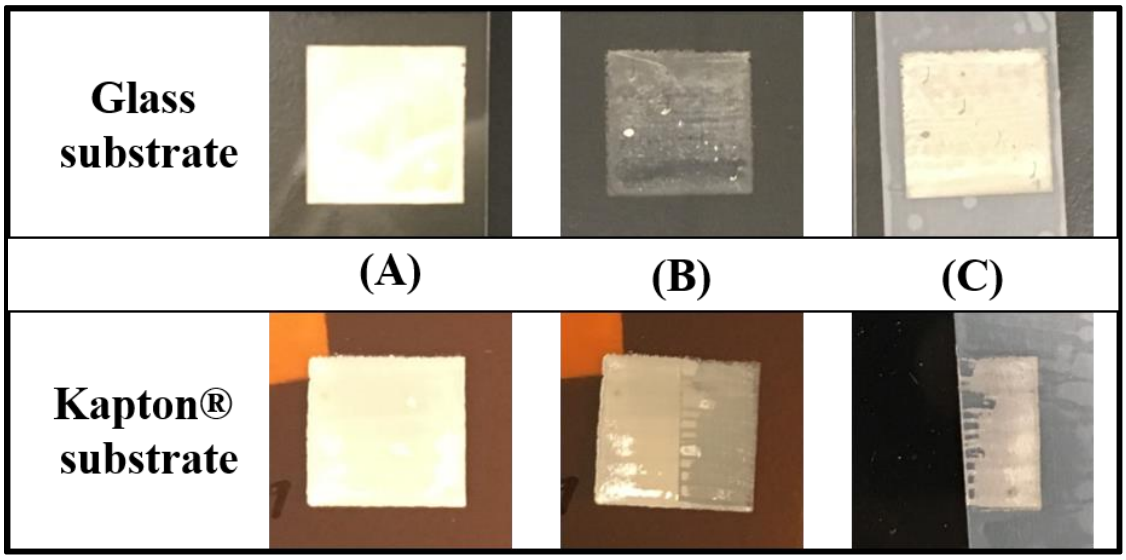

Figure 16: Tape test indicating adhesion and cohesion properties of the printed film. (A) film before the tape test, (B) substrate after the tape test and (C) tape with the film after the test.

Printed films after curing were found to be conductive using a simple two-probe multimeter. More sensitive measurements of the electrical properties of the film using four-point probes will be investigated in future studies.

Chapter 6. Conclusion

A new solid silver (S-Ag) complex was developed for MOD inks used in printed electronics. Inkjet ink formulation of S-Ag complex have been demonstrated in this study. Curing condition for the developed ink were 120° C for less than 5 minutes. Ink formulations of S-Ag complex can also be developed for other ink transfer techniques such as flexography, screen printing or aerosol-jet printing. This solid complex has exhibited good stability when stored in the dark at 4°C.

The proposed S-Ag structure was μ-oxolato-bis(ethylenediaminesilver(I)) as confirmed by thermal analysis as well as NMR and IR spectroscopic characterization. Silver-nitrogen bonded complexes are well known. Isolation of the solid form of the complex, however, has enabled longer shelf life and a wide range of ink formulations. Silver was found to be 46.8% w/w in the S-Ag complex. The combination of a high silver content and high water solubility allowed the formulation of concentrated silver MOD inks. Thermochemical changes during the curing process were analyzed to reveal the last endothermic step at about 120°C. Printing and curing on low-melting substrates, therefore, is be possible.

Printed and optimally cured films were 3.36 μm thick. Elemental and crystallographic analysis of the films indicated that the films were primarily composed of crystalline metallic silver, although recorded electrical conductivity needs further validation. All the components of the ink were thermally degradable at 120°C, leaving behind primarily metallic silver in the film after curing.

Low curing temperature was achieved by designing the S-Ag complex with the optimum amount of organic structure in the complex molecule. Silver oxalate was found to

decompose thermally at 195°C to yield silver and carbon dioxide. Complexation of the silver oxalate molecule was carried out in such a way that a small complexing agent was detached from the silver oxalate molecule first and then helped the reduction to silver at lower temperature. Ethylene diamine not only provides two binding sites for complexing silver salt but also has a relatively low boiling point (below 120°C) assisting rapid curing processes.

Achieving good printability, lower curing temperature and better electrical conductivity have been addressed in many studies in printed electronics. This study has attempted to reduce the existing challenges and limitations of a long processing time and a high curing temperature by developing this new silver-ligand complex.

Chapter 7. Future Work

Further development of ink formulations using solid silver (S-Ag) complex for various other printing processes can be pursued in the future. Curing the printed films was intriguing as the continuous film of liquid ink forms a microstructure of nanoparticles. Annealing of adjacent nanoparticles was important for the film integrity and conductivity. A more detailed study of kinetic-physio-chemical features of the film could lead to improved film integrity without compromising electrical conductivity.

Chapter 8. References

1. Liao, X.; Liao, Q.; Yan, X.; Liang, Q.; Si, H.; Li, M.; Wu, H.; Cao, S.; Zhang, Y., Flexible and highly sensitive strain sensors fabricated by pencil drawn for wearable monitor. *Advanced Functional Materials* **2015,** *25* (16), 2395-2401.

2. Dossi, N.; Terzi, F.; Piccin, E.; Toniolo, R.; Bontempelli, G., Rapid prototyping of sensors and conductive elements by day-to-day writing tools and emerging manufacturing technologies. *Electroanalysis* **2016,** *28* (2), 250-264.

3. Jung, Y.; Yeom, C.; Park, H.; Jung, D.; Koo, H.; Noh, J.; Wang, D. L.; Cho, G., Significant effect of the molecular formula in silver nanoparticle ink to the characteristics of fully gravure-printed carbon nanotube thin-film transistors on flexible polymer substrate. *Organic Electronics* **2016,** *28*, 197-204.

4. Koo, H.; Lee, W.; Choi, Y.; Sun, J.; Bak, J.; Noh, J.; Subramanian, V.; Azuma, Y.; Majima, Y.; Cho, G., Scalability of carbon-nanotube-based thin film transistors for flexible electronic devices manufactured using an all roll-to-roll gravure printing system. *Scientific Reports* **2015,** *5*.

5. Eggenhuisen, T. M.; Galagan, Y.; Coenen, E. W. C.; Voorthuijzen, W. P.; Slaats, M. W. L.; Kommeren, S. A.; Shanmuganam, S.; Coenen, M. J. J.; Andriessen, R.; Groen, W. A., Digital fabrication of organic solar cells by Inkjet printing using non-halogenated solvents. *Solar Energy Materials and Solar Cells* **2015,** *134*, 364-372.

6. Eggenhuisen, T. M.; Galagan, Y.; Biezemans, A. F. K. V.; Slaats, T. M. W. L.; Voorthuijzen, W. P.; Kommeren, S.; Shanmugam, S.; Teunissen, J. P.; Hadipour, A.; Verhees, W. J. H.; Veenstra, S. C.; Coenen, M. J. J.; Gilot, J.; Andriessen, R.; Groen, W.

A., High efficiency, fully inkjet printed organic solar cells with freedom of design. *Journal of Materials Chemistry A* **2015,** *3* (14), 7255-7262.

7. Deol, R. S.; Choi, H. W.; Singh, M.; Jabbour, G. E., Printable displays and light sources for sensor applications: a review. *Ieee Sensors Journal* **2015,** *15* (6), 3186-3195.

8. Yeo, J.; Kim, G.; Hong, S.; Kim, M. S.; Kim, D.; Lee, J.; Lee, H. B.; Kwon, J.; Suh, Y. D.; Kang, H. W.; Sung, H. J.; Choi, J. H.; Hong, W. H.; Ko, J. M.; Lee, S. H.; Choa, S. H.; Ko, S. H., Flexible supercapacitor fabrication by room temperature rapid laser processing of roll-to-roll printed metal nanoparticle ink for wearable electronics application. *Journal of Power Sources* **2014,** *246*, 562-568.

9. Li, J. H.; Xu, L. S.; Tang, C. W.; Shestopalov, A. A., High-resolution organic light-emitting diodes patterned via contact printing. *Acs Applied Materials & Interfaces* **2016,** *8* (26), 16809-16815.

10. Sanchez-Romaguera, V.; Wuenscher, S.; Turki, B. M.; Abbel, R.; Barbosa, S.; Tate, D. J.; Oyeka, D.; Batchelor, J. C.; Parker, E. A.; Schubert, U. S.; Yeates, S. G., Inkjet printed paper based frequency selective surfaces and skin mounted RFID tags: the interrelation between silver nanoparticle ink, paper substrate and low temperature sintering technique. *Journal of Materials Chemistry C* **2015,** *3* (9), 2132-2140.

11. Ankireddy, K.; Menon, A. K.; Iezzi, B.; Yee, S. K.; Losego, M. D.; Jur, J. S., Electrical conductivity, thermal behavior, and seebeck coefficient of conductive films for printed thermoelectric energy harvesting systems. *Journal of Electronic Materials* **2016,** *45* (11), 5561-5569.

12. Choi, H. W.; Zhou, T.; Singh, M.; Jabbour, G. E., Recent developments and directions in printed nanomaterials. *Nanoscale* **2015,** *7* (8), 3338-3355.

13. Rogers, J. A.; Someya, T.; Huang, Y., Materials and mechanics for stretchable electronics. *Science* **2010,** *327* (5973), 1603-1607.

14. Sondergaard, R. R.; Hosel, M.; Krebs, F. C., Roll-to-roll fabrication of large area functional organic materials. *Journal of Polymer Science Part B-Polymer Physics* **2013,** *51* (1), 16-34.

15. Kahn, B. E., Patterning processes for flexible electronics. *Proceedings of the Ieee* **2015,** *103* (4), 497-517.

16. Rim, Y. S.; Bae, S.-H.; Chen, H.; De Marco, N.; Yang, Y., Recent progress in materials and devices toward printable and flexible sensors. *Advanced Materials* **2016,** *28* (22), 4415-4440.

17. Aleeva, Y.; Pignataro, B., Recent advances in upscalable wet methods and ink formulations for printed electronics. *Journal of Materials Chemistry C* **2014,** *2* (32), 6436-6453.

18. Teng, K. F.; Vest, R. W., Liquid ink jet printing with MOD inks for hybrid microcircuits. *Ieee Transactions on Components Hybrids and Manufacturing Technology* **1987,** *10* (4), 545-549.

19. Yang, C.; Wong, C. P.; Yuen, M. M. F., Printed electrically conductive composites: conductive filler designs and surface engineering. *Journal of Materials Chemistry C* **2013,** *1* (26), 4052-4069.

20. Lai, C. Y.; Cheong, C. F.; Mandeep, J. S.; Abdullah, H. B.; Amin, N.; Lai, K. W., Synthesis and characterization of silver nanoparticles and silver inks: review on the past and recent technology roadmaps. *Journal of Materials Engineering and Performance* **2014,** *23* (10), 3541-3550.

21. Rao, V. K. R.; Abhinav, V. K.; Karthik, P. S.; Singh, S. P., Conductive silver inks and their applications in printed and flexible electronics. *Rsc Advances* **2015,** *5* (95), 77760-77790.

22. Dong, Y.; Li, X. D.; Liu, S. H.; Zhu, Q.; Li, J. G.; Sun, X. D., Facile synthesis of high silver content MOD ink by using silver oxalate precursor for inkjet printing applications. *Thin Solid Films* **2015,** *589*, 381-387.

23. Lin, H. C.; Lin, P.; Lu, C. A.; Wang, S. F., Effects of silver oxalate additions on the physical characteristics of low-temperature-curing MOD silver paste for thick-film applications. *Microelectronic Engineering* **2009,** *86* (11), 2316-2319.

24. Walker, S. B.; Lewis, J. A., Reactive silver inks for patterning high-conductivity features at mild temperatures. *Journal of the American Chemical Society* **2012,** *134* (3), 1419-1421.

25. Farraj, Y.; Grouchko, M.; Magdassi, S., Self-reduction of a copper complex MOD ink for inkjet printing conductive patterns on plastics. *Chemical Communications* **2015,** *51* (9), 1587-1590.

26. Capasso, A.; Castillo, A. E. D. R.; Sun, H.; Ansaldo, A.; Pellegrini, V.; Bonaccorso, F., Ink-jet printing of graphene for flexible electronics: An environmentally-friendly approach. *Solid State Communications* **2015,** *224*, 53-63.

27. Li, J. H.; Xu, L. S.; Tang, C. W.; Shestopalov, A. A., High-resolution organic light-emitting diodes patterned via contact printing. *Acs Applied Materials & Interfaces* **2016,** *8* (26), 16809-16815.

28. Berggren, M.; Nilsson, D.; Robinson, N. D., Organic materials for printed electronics. *Nature Materials* **2007,** *6* (1), 3-5.

29. Li, Y. N., Development of high performance materials for printed organic electronics. *Abstracts of Papers of the American Chemical Society* **2011,** *242*.

30. Liana, D. D.; Raguse, B.; Gooding, J. J.; Chow, E., Recent advances in paper-based sensors. *Sensors* **2012,** *12* (9), 11505-11526.

31. Vaillancourt, J.; Zhang, H.; Vasinajindakaw, P.; Xia, H.; Lu, X.; Han, X.; Janzen, D. C.; Shih, W.-S.; Jones, C. S.; Stroder, M.; Chen, M. Y.; Subbaraman, H.; Chen, R. T.; Berger, U.; Renn, M., All ink-jet-printed carbon nanotube thin-film transistor on a polyimide substrate with an ultrahigh operating frequency of over 5 GHz. *Applied Physics Letters* **2008,** *93* (24).

32. Wu, J. T.; Hsu, S. L. C.; Tsai, M. H.; Hwang, W. S., Inkjet printing of low-temperature cured silver patterns by using AgNO3/1-Dimethylamino-2-propanol inks on polymer substrates. *Journal of Physical Chemistry C* **2011,** *115* (22), 10940-10945.

33. Loffelmann, U.; Korvink, J. G.; Hendriks, C. E.; Schubert, U. S.; Smith, P. J., Ink jet printed silver lines formed in microchannels exhibit lower resistance than their unstructured counterparts. *Journal of Imaging Science and Technology* **2011,** *55* (4), 6.

34. Perelaer, J.; Hendriks, C. E.; de Laat, A. W. M.; Schubert, U. S., One-step inkjet printing of conductive silver tracks on polymer substrates. *Nanotechnology* **2009,** *20* (16), 5.

35. Dearden, A. L.; Smith, P. J.; Shin, D. Y.; Reis, N.; Derby, B.; O'Brien, P., A low curing temperature silver ink for use in ink-jet printing and subsequent production of conductive tracks. *Macromolecular Rapid Communications* **2005,** *26* (4), 315-318.

36. Mei, J. F.; Lovell, M. R.; Mickle, M. H., Formulation and processing of novel conductive solution inks in continuous inkjet printing of 3-D electric circuits. *Ieee Transactions on Electronics Packaging Manufacturing* **2005,** *28* (3), 265-273.

37. Jahn, S. F.; Jakob, A.; Blaudeck, T.; Schmidt, P.; Lang, H.; Baumann, R. R., Inkjet printing of conductive patterns with an aqueous solution of AgO2C(CH2OCH2)(3)H without any additional stabilizing ligands. *Thin Solid Films* **2010,** *518* (12), 3218-3222.

38. Grouchko, M.; Kamyshny, A.; Mihailescu, C. F.; Anghel, D. F.; Magdassi, S., Conductive inks with a "built-in" mechanism that enables sintering at room temperature. *Acs Nano* **2011,** *5* (4), 3354-3359.

39. Black, K.; Singh, J.; Mehta, D.; Sung, S.; Sutcliffe, C. J.; Chalker, P. R., Silver ink formulations for sinter-free printing of conductive films. *Scientific Reports* **2016,** *6*.

40. Boldyrev, V. V., Thermal decomposition of silver oxalate. *Thermochimica Acta* **2002,** *388* (1-2), 63-90.

41. Nie, X.; Wang, H.; Zou, J., Inkjet printing of silver citrate conductive ink on PET substrate. *Applied Surface Science* **2012,** *261*, 554-560.

42. De Volder, M. F. L.; Tawfick, S. H.; Baughman, R. H.; Hart, A. J., Carbon nanotubes: present and future commercial applications. *Science* **2013,** *339* (6119), 535-539.

43. Takahashi, T.; Yu, Z. B.; Chen, K.; Kiriya, D.; Wang, C.; Takei, K.; Shiraki, H.; Chen, T.; Ma, B. W.; Javey, A., Carbon nanotube active-matrix backplanes for mechanically flexible visible light and x-ray imagers. *Nano Letters* **2013,** *13* (11), 5425-5430.

44. Gruner, G., Printed electronics, wearable technology. *Translational Materials Research* **2016,** *3* (3).

45. Suren, S.; Limkitnuwat, W.; Benjapongvimon, P.; Kheawhom, S., Conductive film by spray pyrolysis of self-reducing copper-silver amine complex solution. *Thin Solid Films* **2016,** *607*, 36-42.

46. Angmo, D.; Andersen, T. R.; Bentzen, J. J.; Helgesen, M.; Sondergaard, R. R.; Jorgensen, M.; Carle, J. E.; Bundgaard, E.; Krebs, F. C., Roll-to-roll printed silver nanowire semitransparent electrodes for fully ambient solution-processed tandem polymer solar cells. *Advanced Functional Materials* **2015,** *25* (28), 4539-4547.

47. Chang, Y.; Wang, D. Y.; Tai, Y. L.; Yang, Z. G., Preparation, characterization and reaction mechanism of a novel silver-organic conductive ink. *Journal of Materials Chemistry* **2012,** *22* (48), 25296-25301.

48. Tao, Y.; Tao, Y. X.; Wang, B. B.; Wang, L. Y.; Tai, Y. L., A facile approach to a silver conductive ink with high performance for macroelectronics. *Nanoscale Research Letters* **2013,** *8*, 1-6.

49. Li, S.; Liu, P.; Wang, Q. S.; Chen, X.; Ieee, Preparation of stable aqueous based Ag nanoparticle ink with different capping agent for printing on a plastic substrate. *Proceedings of the 2012 Ieee 14th Electronics Packaging Technology Conference* **2012**, 740-743.

50. Li, Y. N.; Wu, Y. L.; Ong, B. S., Facile synthesis of silver nanoparticles useful for fabrication of high-conductivity elements for printed electronics. *Journal of the American Chemical Society* **2005,** *127* (10), 3266-3267.

51. Grouchko, M.; Kamyshny, A.; Magdassi, S., Formation of air-stable copper-silver core-shell nanoparticles for inkjet printing. *Journal of Materials Chemistry* **2009,** *19* (19), 3057-3062.

52. Cahill, V.; Taylor, D.; Is, Evaluation of inkjet technologies for digital fabrication & functional printing. *Nip28: 28th International Conference on Digital Printing Technologies / Digital Fabrication 2012* **2012**, 315-317.

53. Hutchings, I. M.; Martin, G.; Ebook, L.; Books24x, I., *Inkjet technology for digital fabrication*. John Wiley & Sons Ltd: Chichester, West Sussex, United Kingdom, 2013; Vol. 1. Aufl.;1;.

54. Tekin, E.; Smith, P. J.; Schubert, U. S., Inkjet printing as a deposition and patterning tool for polymers and inorganic particles. *Soft Matter* **2008,** *4* (4), 703-713.

55. Navaladian, S.; Viswanathan, B.; Viswanath, R. P.; Varadarajan, T. K., Thermal decomposition as route for silver nanoparticles. *Nanoscale Research Letters* **2007,** *2* (1), 44-48.

56. Sarada, K.; Vijisha, K. R.; Muraleedharan, K., Exploration of the thermal decomposition of oxalates of copper and silver by experimental and computational methods. *Journal of Analytical and Applied Pyrolysis* **2016,** *120,* 207-214.

57. Fujita, J.; Nakamoto, K.; Kobayashi, M., Infrared spectra of metallic complexes .3. The infrared spectra of metallic oxalates. *Journal of Physical Chemistry* **1957,** *61* (7), 1014-1015.

58. Feltham, P., Science of engineering materials. *British Journal of Applied Physics* **1966,** *17* (6), 836-840;.

59. ASTM D3359-09e2, Standard Test Methods for Measuring Adhesion by Tape Test. ASTM International, West Conshohocken, PA: http://www.astm.org/cgi-bin/resolver.cgi?D3359, 2009.